Technical Note

4D Time-Resolved MR Angiography With Keyhole (4D-TRAK): More Than 60 Times Accelerated MRA Using a Combination of CENTRA, Keyhole, and SENSE at 3.0T

Winfried A. Willinek, MD,[1]* Dariusch R. Hadizadeh, MD,[1] Marcus von Falkenhausen, MD,[1] Horst Urbach, MD,[1] R. Hoogeveen, MD, PhD,[2] Hans H. Schild, MD,[1] and Jürgen Gieseke, PhD[1,2]

Purpose: To present a new 4D method that is designed to provide high spatial resolution MR angiograms at subsecond temporal resolution by combining different techniques of view sharing with parallel imaging at 3.0T.

Materials and Methods: In the keyhole-based method, a central elliptical cylinder in *k*-space is repeated *n* times (keyhole) with a random acquisition (CENTRA), and followed by the readout of the periphery of *k*-space. 4D-MR angiography with CENTRA keyhole (4D-TRAK) was combined with parallel imaging (SENSE) and partial Fourier imaging. In total, a speed-up factor of 66.5 (6.25 [CENTRA keyhole] × 8 [SENSE] × 1.33 [partial Fourier imaging]) was achieved yielding a temporal resolution of 608 ms and a spatial resolution of $(1.1 \times 1.4 \times 1.1)$ mm^3 with whole-brain coverage 4D-TRAK was applied to five patients and compared with digital subtraction angiography (DSA).

Results: 4D-TRAK was successfully completed with an acceleration factor of 66.5 in all five patients. Sharp images were acquired without any artifacts possibly created by the transition of the central cylinder and the reference dataset. MRA findings were concordant with DSA.

Conclusion: 4D time-resolved MRA with keyhole (4D-TRAK) is feasible using a combination of CENTRA, keyhole, and SENSE at 3.0T and allows for more than 60 times accelerated MRA with high spatial resolution.

Key Words: time-resolved MRA; 4-dimensional; keyhole; 3 Tesla; parallel imaging
J. Magn. Reson. Imaging 2008;27:1455–1460.

CONTRAST-ENHANCED MR angiography (MRA) is routinely used for imaging of the vascular system in many centers (1,2). Although techniques of contrast-enhanced MRA have continuously improved in the past, there is still a demand for acquiring both high spatial resolution and high temporal resolution at the same time, as is achieved in single projection techniques such as digital subtraction angiography (DSA). It has been demonstrated that very high spatial resolution images without venous contamination can be obtained in contrast-enhanced MRA of the supraaortic arteries by starting to acquire phase-encoding in or near the center of *k*-space (elliptical centric (3) / CENTRA (4)). Nevertheless, these methods primarily do not contain dynamic information. Additional dynamic information, however, is clinically required or at least desired in many MRA applications (eg, MRA of cerebral arteriovenous malformations [cAVM], MRA of the foot, MRA of hemodialysis shunts, etc) to allow insight into filling and outflow of the contrast agent in the vessels. In this study a new method is presented which is designed to provide 4D contrast-enhanced MRA with high spatial resolution and more than 60 times accelerated temporal resolution by combining CENTRA with the keyhole method (5), partial Fourier, and SENSE (6) at 3.0T. In addition, an update of the literature on time-resolved MRA is given and our method is compared to currently available techniques of time-resolved MRA.

MATERIALS AND METHODS

Patient Studies

Between April and September 2005, five patients (two men, three women; age range: 23–59 years, mean age: 35 years) were included in this feasibility study. All patients presented with cerebral arteriovenous malformations. Age below 18 years and contraindication to MR imaging (ie, pacemakers, metallic implants, etc) or inability to give written informed consent were exclusion criteria. The study protocol was approved by our Institutional Review Board and written informed consent was obtained from all patients. All patients re-

[1]Department of Radiology, University of Bonn, Germany.
[2]Philips Medical Systems, Best, the Netherlands.
Presented in part at the 14th ISMRM Scientific Meeting & Exhibition 2006, Seattle, Washington.
Winfried A. Willinek and Dariusch R. Hadizadeh contributed equally to this work.
*Address reprint requests to: W.A.W., Department of Radiology, University of Bonn, Sigmund-Freud-Strasse 25, D-53105 Bonn, Germany. E-mail: winfried.willinek@ukb.uni-bonn.de
Received April 2, 2007; Accepted February 6, 2008.
DOI 10.1002/jmri.21354
Published online in Wiley InterScience (www.interscience.wiley.com).

ceived DSA during diagnostic work-up and these DSA images were available for comparison. The patients underwent MR angiography and conventional angiography within 16 days.

MR Imaging

Contrast-enhanced MR angiography was performed on a 32-channel 3.0T Achieva system (Philips Medical Systems, Best, The Netherlands) equipped with a commercially available eight-channel SENSE capable head coil. The gradient system of the MR unit allows a maximal achievable gradient amplitude of 80 mT/m with a rise time of 0.2 msec and a slew rate of 200 T/m/s.

An automated power injector (Spectris; Medrad Europe, Beek, The Netherlands) was used for a biphasic injection protocol. Ten mL of gadopentate dimeglumine (Gd-DTPA, Magnevist; Schering, Berlin, Germany) were injected initially at a flow rate of 3 mL/s followed by 10 mL Gd-DTPA at a flow rate of 1.5 mL/s and by a saline flush of 25 mL at a flow rate of 1.5 mL/s. The 4D MRA sequence was started 10 seconds after the beginning of the injection.

4D-TRAK was acquired using the keyhole method (5,7), partial Fourier, and CENTRA (4) with 16% of the *k*-space in k_y and in k_z directions which were uploaded for every keyhole frame. In CENTRA, a central k_yk_z-space cylinder is randomly filled allowing for *k*-space sampling during the whole passage of the contrast bolus over time (4). CENTRA keyhole imaging with a portion of 16% of the reference dataset (ie, 40% of the full 3D *k*-space) allowed for an acceleration factor (AF) of 6.25 compared with non-keyhole acquisition. The periphery of *k*-space was collected in the reference dataset at the end of the acquisition in an elliptical order and the resulting data were used for reconstruction of each of the dynamic phases as described in the keyhole approach (5,7). In addition to the CENTRA keyhole method, parallel imaging was implemented in the 4D-TRAK protocol. Sensitivity encoding (SENSE) was used with a reduction factor of 4 in the phase-encoding direction and a reduction factor of 2 in the slice-encoding direction yielding a total AF of 8 (6). Furthermore, partial Fourier imaging was added skipping 25% of *k*-space, accelerating the *k*-space sampling by a factor of 1.33. Combining these techniques, 4D-TRAK yielded a total acceleration of $6.25 \times 8 \times 1.33 = 66.5$ as compared to standard 3D MRA techniques without these methods.

The acquisition parameters of the 4D-TRAK sequence were the following: T1-weighted gradient-echo-sequence with TR = 2.2, TE = 0.9, flip angle = 15°, rectangular field of view 100%, a slab thickness of 154 mm, and an image matrix of 224×178 over a 256 mm field of view with 140 thin partitions of 2.2 mm with 1.1 mm overlap (interpolation factor 2) and an oversampling factor of 1.4 in k_y direction, yielding an almost isotropic voxel size of $(1.1 \times 1.4 \times 1.1)$ mm^3 before zero-filling. First, a native mask scan was acquired to allow for complex subtraction of the stationary tissue, followed by 49 dynamic samples that were acquired at a temporal resolution of 608 msec/dynamic scan ([Number of phase-encoding steps k_y / SENSE factor k_y] * partial Fourier * [Number of phase encoding steps k_z / SENSE factor k_z] * [oversampling factor / interpolation factor] * [keyhole %/100] * TR) and the reference dataset. Total acquisition time of 4D-TRAK was 37.4 seconds including 3.8 seconds for the acquisition of the reference dataset. Subtracted MR angiographic data were available on a separate workstation (Viewforum Release 5.1, Philips Medical Systems) for postprocessing to allow for multiple projection reformats (MPR) and maximum intensity projections (MIP) of the 3D datasets. A "cine" function of the workstation display enabled dynamic visualization of the acquired data (4D).

Catheter Angiography

DSA was performed on a biplane Integris V 5000 (Philips Medical Systems) with a 5F catheter that was navigated into the internal carotid, external carotid, and vertebral arteries via the transfemoral route in 5/5 patients. The images were acquired after manual injection of 5–7 mL of iopromide (Ultravist, Schering, Germany). Frame rates were 3/second in the arterial phase, 2/second in the venous phase, and 8 frames/second in the fast angiographic series.

Image Evaluation

Both DSA and MRA were independently reviewed at different times by two experienced readers (W.W., H.U.; both >6 years of experience). The readers were blinded to the patient names, their clinical histories, and results of other diagnostic procedures. First, the readers were asked to indicate whether differentiation into early arterial, late arterial, early venous, and late venous phases was possible ("Yes/No").

Second, overall diagnostic quality of the 4D-TRAK images was scored according to the following 4-point grading system. 4: Excellent, if feeding and draining vessels were clearly depicted and no or only subtle contrast enhancement was preexisting in the first dynamic image and image quality was not impaired by artifacts. 3: Adequate for diagnosis, if depiction of feeding arteries and draining veins was possible, but contrast enhancement was preexisting in the first dynamic image and minor artifacts were present, but did not interfere with image interpretation. 2: Questionable for diagnosis, if depiction of feeding arteries and draining veins was impaired by contrast enhancement preexisting in the first dynamic image and/or artifacts. 1: Nondiagnostic, if image quality was not sufficient for diagnosing feeding arteries and draining veins because of contrast enhancement preexisting in the first dynamic image and/or artifacts.

Because of the complex method of *k*-space ordering that was implemented in the pulse sequence (including CENTRA, partial Fourier, SENSE, and keyhole), particular attention was given to the presence of periodic SENSE artifacts and/or ringing artifacts in the evaluation of image quality.

In a third step, both readers were asked to indicate the number and the exact localization of arterial feeders and draining veins of the AVMs by reviewing the volumetric 4D-TRAK datasets on the workstation as well as the DSA images on hard copies.

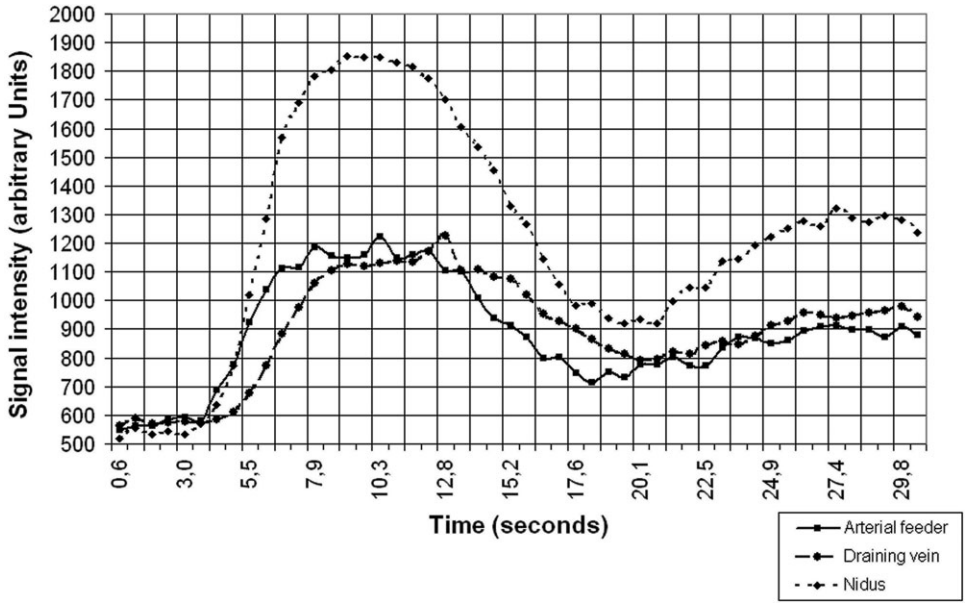

Figure 1. Signal intensity over time curve displaying the enhancement of the feeding artery and draining vein of a left parasagittal cAVM (nidus size: 2.7 cm) in a 23-year-old female (see Fig. 3).

A region-of-interest (ROI) was drawn in the nidus and in the arterial feeder and the draining vein as close as possible to nidus on one series and copied to the remaining series. The mean of 30 pixels (30 mm^3) was used to estimate the intensity/time curve. All ROI measurements were made by the same author (D.H.; >3 years of experience).

Statistical Analysis

The Kendall W coefficient of concordance was computed to compare the two readers in their assessments of image quality as well as the depiction of feeding arteries and veins as determined by 4D-TRAK and DSA. Kendall W coefficients between 0.5 and 0.8 were considered to indicate good agreement and coefficients higher than 0.8 were considered to indicate excellent agreement. All statistical analyses were performed with SPSS v. 11.0 (SPSS, Chicago, IL). As only five patients were included in this technical feasibility study, the importance of the statistical conclusions is limited.

RESULTS

4D-TRAK was successfully completed in five out of five (100%) patients. The 3D volumetric datasets providing both high spatial and high temporal resolution allowed for differentiation of early arterial, late arterial, early venous, and late venous phases in all cases as indicated by both readers' ratings (5/5 "Yes" and 0/0 "No," respectively). Figure 1 displays the contrast over time curves for the arterial feeders, the nidus and the draining vein in a patient with a left parasagittal AVM with a nidus size of 2.7 cm. Figure 2 shows one example of some of the essential dynamic frames of 4D-TRAK in a patient with left occipital cAVM.

Image quality of 4D-TRAK was judged by both readers to be excellent in all patients (4.0 ± 0) with excellent interobserver agreement (K = 1). Periodical SENSE artifacts and ringing artifacts were not seen in any of the cases. No other artifacts were present in five case studies. The temporal (608 msec) and spatial resolution ([1.1 × 1.4 × 1.1] mm^3 = 1.7 mm^3) of 4D-TRAK is listed in Table 1 and compared with dynamic MRA approaches in the literature (2D MRA, Table 2; 3D MRA, Table 3).

Deep venous drainage was present in 4/5 patients, whereas in 1/5 of the patients only superficial veins were involved in the drainage of the cAVM. The identi-

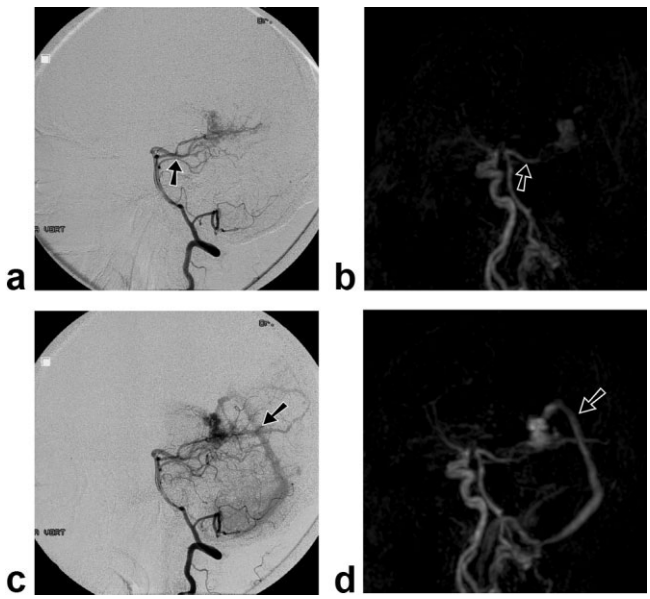

Figure 2. Two dynamic phases (**b,d;** maximum intensity projections; sagittal) of the 3D T1-weighted gradient echo sequence provided by 4D-TRAK displaying the arterial feeder (posterior cerebral artery; **a,b:** arrows) and the venous drainage (straight sinus; **c,d:** arrows) of a left occipital cAVM (nidus size: 2.5 cm) in a 59-year-old male as compared to corresponding phases of lateral views of DSA (a,c) after selective catheterization of the left vertebral artery.

Table 1
Spatial and Temporal Resolution of 4D Time-Resolved MRA With Keyhole, CENTRA, and SENSE

Study	*n*	FS	Spatial Resolution	T
4D-TRAK	5	3.0T	(1.1 x 1.4 x 1.1) mm^3	0.608 s

n = number of individuals examined in the study; FS = field strength of magnet used for imaging; t = temporal resolution as time needed for each dynamic scan.

fication of venous drainage patterns of cAVM (deep/superficial) using 4D-TRAK matched with DSA in 5/5 patients for both readers (100%) yielding a 100% inter-observer agreement (K = 1). The arterial feeders as depicted by 4D-TRAK were as follows: anterior cerebral artery (*n* = 3) (Fig. 3), middle cerebral artery (*n* = 3), posterior cerebral artery (*n* = 2). All arterial feeders were confirmed by DSA.

DISCUSSION

To our knowledge, this is the first study to address a combination of CENTRA, keyhole, partial Fourier, and SENSE for 4D time-resolved MRA at 3.0T yielding a total acceleration factor more than 60. Due to the short time of contrast media passage through the whole brain, the total scan time is limited to obtain reliable temporal information. Consequently, the reference scan (acquisition of the reference dataset) must be kept as short as possible to maintain high temporal resolution at high spatial resolution without false registration of the temporal information. This can be achieved with the application of SENSE and partial Fourier in addition to keyhole imaging with a 3D *k*-space fraction of 16% (ie, *k*-space diameter of 40%) yielding an acceleration factor of 6.25. While the data acquisition is truly accelerated by the use of SENSE (8 times accelerated) and the use of partial Fourier (1.33 times accelerated), it is important to notice that the keyhole method accelerates the dynamic imaging, but is object-dependent. Objects that are smaller than the spatial resolution of the keyhole fraction may only be visualized with the help of higher spatial frequencies that are acquired during the reference scan. The results of this study indicate the feasibility of the combination of CENTRA, keyhole, partial Fourier, and SENSE and the clinical application to MRA of cAVMs.

DSA still is considered the standard of reference for diagnosis of arteriovenous malformations with typically short arteriovenous transit times because of the very high temporal and high spatial resolution that is inherent to DSA (8,9). Since 1993, when contrast-enhanced MRA was first introduced by Prince et al (10), there has always been a trade-off in clinical practice between spatial and temporal resolution of MRA. More recently, several techniques for time-resolved 3D MRA were published with a maximum temporal resolution of 1.5 s/dynamic scan (11–16). However, spatial resolution in these reports was much lower than the acquired ($1.1 \times 1.4 \times 1.1$) mm^3 that was achieved with our study protocol (Table 3). It is well known that 2D single thick slice techniques of time-resolved MRA can achieve very high temporal resolution (17–21), but at the expense of spatial resolution (Table 2). Furthermore, postprocessing potentials inherent to a full 3D dataset are not available using these methods.

Parallel imaging (PI), echo-sharing, and high field imaging are reported to be a very favorable combination to accelerate the temporal resolution of contrast-enhanced MRA (13,16,18,20,22,23). As PI acceleration factors are limited at 1.5T because of signal-to-noise (SNR) issues, the promise at 3.0T is the use of higher PI acceleration factors through the improved SNR and the use of dedicated receiver coil arrays: PI acceleration factors of more than 8 have already been successfully implemented on whole-body 3.0T systems (24). The application of PI especially with a high PI factor is known to cause a loss in SNR, which was well compensated in our study with the high field strength of 3.0T. In addition, PI artifacts are reduced with oversampling in the phase-encoding direction and were not seen in our study.

Randomly segmented central *k*-space ordering (CENTRA) proved to allow for robust arterial phase MRA of the supraaortic arteries despite acquisition times of more than 1 minute (4,25). Keyhole imaging in MRI was first published in 1993 by Van Vaals et al (5) and Jones et al (7). However, it seems that this method gains increasing interest only today with the advent of both PI and high field scanners. Despite the well-known limitations of each of the techniques, the combination of them seems to be advantageous especially at a field strength of 3.0T (20,26). The known limitations of keyhole imaging including amplitude and phase discontinuities, as described in applications such as T2*-weighted perfusion imaging and keyhole functional imaging, are mostly related to long echo times (27,28). However, these limitations can be overcome by using 3D gradient echo sequences with very short echo times. The successful combination of keyhole and parallel imaging in the phase-encoding direction has recently been shown

Table 2
Studies on High Temporal Resolution 2-Dimensional Single Frame MR Angiography in Patients With cAVM

Study	*n*	FS	Spatial Resolution	T
Warren et al. 2001 (21)	40	1.5T	(0.90 x 1.53 x 60-100) mm^3	1 s
Mori et al. 2003 (18)	55	1.5T	(0.47 x 1.25 x 70-80) mm^3	1.05 s
Summers et al. 2004 (20)	19	3.0T	(0.60 x 1.00 x 50-80) mm^3	0.167 – 1 s
Nagaraja et al. 2005 (19)	60	1.5T	(0.90 x 1.53 x 60-100) mm^3	1 s
Hans et al. 2005 (17)	12	1.5T	(1.08 x 0.90 x 50-150) mm^3	0.34 – 1 s

n = number of individuals examined in the study; FS = field strength of magnets used for imaging; t = temporal resolution as time needed for each dynamic scan.

Table 3
Studies on High Temporal Resolution 3D-MR Angiography in Patients With cAVM

Study	*n*	FS	Spatial Resolution	T
Farb et al 2001 (12)	10	1.5T	(0.625 x 1.5625 x 10) mm^3	1.5 s
Duran et al 2002 (11)	22	1.5T	matrix size: 128 x 256 (FOV missing)	9 s
Tsuchiya et al 2004 (14)	2	1.5T	(1.22 – 1.67 x 0.49 – 0.55 x 7.5) mm^3	1.68 s
Wu et al 2004 (15)	24	1.5T	(0.6 x 0.6 x 1.5) mm^3	2.9 s
Gauvrit et al 2006 (13)	54	1.5T	(0.9375 x 1.562 x 10) mm^3	1.7 s
Ziyeh et al 2005 (16)	3	3.0T	(0.8 x 0.8 x 0.6) mm^3	1.5 s
Nael et al 2006 (22)	3	3.0T	(1.3 x 1.0 x 4.3) mm^3	1.8 s

n = number of individuals examined in the study; FS = field strength of magnets used for imaging; FOV = field of view; t = temporal resolution as time needed for each dynamic scan.

at a field strength of 1.5T in patients with hemodialysis shunts (29).

Furthermore, a relatively high spatial resolution of ≈4.3 mm^3 can be obtained in the "low-resolution" dynamic keyhole images due to the implementation of keyhole in both k_y and k_z directions, as shown in our study. According to the spatial resolution reported in this study, the keyhole frames should contain dynamic information even of small vessels. Of course, higher isotropic spatial resolution would probably improve the correct spatial representation of even smaller structures with reliable dynamic information. However, it was not the aim of this study to determine the minimal vessel size that would allow for correct depiction within the dynamic frames, but to evaluate the feasibility of the combination of different techniques for acceleration of time-resolved imaging and to test its clinical application. In the future, mathematical simulations with respect to different keyhole parameters and contrast material flow conditions as well as further experiments including vessel phantoms are needed and are under way to define the limits in spatial and temporal representation.

3D-TRICKS (30,31) and TREAT (32) are other methods that undersample *k*-space to acquire high temporal resolution. However, in TRICKS the prediction of artifacts might be much more challenging, especially with contrast injections using flow rates of 4 mL/s and higher (33). The random sampling of central *k*-space in 4D-TRAK may contribute to a smoother transition of the contrast bolus.

Further studies in a larger patient group are needed to evaluate the clinical performance of 4D-TRAK in comparison with DSA. In addition to the evaluation of arteriovenous malformations of the brain, potential applications of 4D-TRAK include time-resolved imaging of

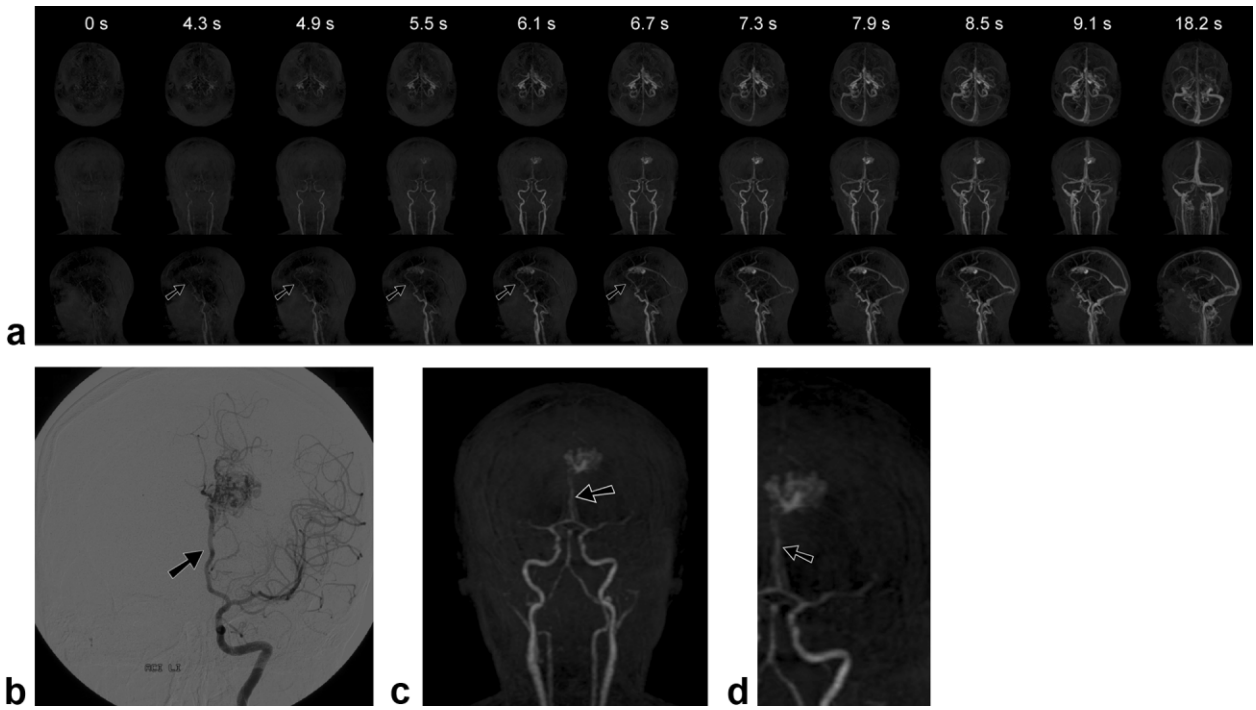

Figure 3. Depiction of the arterial feeder (pericallosal artery, arrow) of a left parasagittal cAVM (nidus size: 2.7 cm) in a 23-year-old female as visualized in 11 of 50 dynamic phases (maximum intensity projections; transverse, upper row; coronal, middle row; sagittal, lower row) of the 3D T1-weighted gradient echo sequence provided by 4D-TRAK (**a**, magnified: **c**,**d**), and in the arterial phase of DSA (a.p. view) after selective catheterization of the left common carotid artery (**b**), confirming the arterial feeder from the anterior cerebral artery (arrow).

hemodialysis shunts and imaging of vessels of the feet, hand, and pulmonary vessels.

In conclusion, 4D time-resolved MR angiography with keyhole (4D-TRAK) is feasible using a combination of CENTRA, partial Fourier, SENSE, and keyhole at 3.0T. 4D-TRAK allows for more than 60 times accelerated MRA with high spatial resolution and allows for proper detection of large arterial feeders and draining veins. The diagnostic impact of this promising technique especially with respect to the identification of small vessels should be investigated in a larger clinical trial.

REFERENCES

1. Huston J III, Fain SB, Wald JT, et al. Carotid artery: elliptic centric contrast-enhanced MR angiography compared with conventional angiography. Radiology 2001;218:138–143.
2. Willinek WA, von Falkenhausen M, Born M, et al. Noninvasive detection of steno-occlusive disease of the supra-aortic arteries with three-dimensional contrast-enhanced magnetic resonance angiography: a prospective, intra-individual comparative analysis with digital subtraction angiography. Stroke 2005;36:38–43.
3. Wilman AH, Riederer SJ, Huston J III, Wald JT, Debbins JP. Arterial phase carotid and vertebral artery imaging in 3D contrast-enhanced MR angiography by combining fluoroscopic triggering with an elliptical centric acquisition order. Magn Reson Med 1998; 40:24–35.
4. Willinek WA, Gieseke J, Conrad R, et al. Randomly segmented central k-space ordering in high-spatial-resolution contrast-enhanced MR angiography of the supraaortic arteries: initial experience. Radiology 2002;225:583–588.
5. van Vaals JJ, Brummer ME, Dixon WT, et al. "Keyhole" method for accelerating imaging of contrast agent uptake. J Magn Reson Imaging 1993;3:671–675.
6. Pruessmann KP, Weiger M, Scheidegger MB, Boesiger P. SENSE: sensitivity encoding for fast MRI. Magn Reson Med 1999;42:952–962.
7. Jones RA, Haraldseth O, Muller TB, Rinck PA, Oksendal AN. K-space substitution: a novel dynamic imaging technique. Magn Reson Med 1993;29:830–834.
8. Fasulakis S, Andronikou S. Comparison of MR angiography and conventional angiography in the investigation of intracranial arteriovenous malformations and aneurysms in children. Pediatr Radiol 2003;33:378–384.
9. Wintermark M, Dillon WP. Advanced CT and MR imaging techniques: an academic whim or a clinical standard in the making? AJNR Am J Neuroradiol 2006;27:1257.
10. Prince MR, Yucel EK, Kaufman JA, Harrison DC, Geller SC. Dynamic gadolinium-enhanced three-dimensional abdominal MR arteriography. J Magn Reson Imaging 1993;3:877–881.
11. Duran M, Schoenberg SO, Yuh WT, Knopp MV, van Kaick G, Essig M. Cerebral arteriovenous malformations: morphologic evaluation by ultrashort 3D gadolinium-enhanced MR angiography. Eur Radiol 2002;12:2957–2964.
12. Farb RI, McGregor C, Kim JK, et al. Intracranial arteriovenous malformations: real-time auto-triggered elliptic centric-ordered 3D gadolinium-enhanced MR angiography—initial assessment. Radiology 2001;220:244–251.
13. Gauvrit JY, Oppenheim C, Nataf F, et al. Three-dimensional dynamic magnetic resonance angiography for the evaluation of radiosurgically treated cerebral arteriovenous malformations. Eur Radiol 2006;16:583–591.
14. Tsuchiya K, Aoki C, Fujikawa A, Hachiya J. Three-dimensional MR digital subtraction angiography using parallel imaging and keyhole data sampling in cerebrovascular diseases: initial experience. Eur Radiol 2004;14:1494–1497.
15. Wu Y, Goodrich KC, Buswell HR, Katzman GL, Parker DL. High-resolution time-resolved contrast-enhanced 3D MRA by combining SENSE with keyhole and SLAM strategies. Magn Reson Imaging 2004;22:1161–1168.
16. Ziyeh S, Strecker R, Berlis A, Weber J, Klisch J, Mader I. Dynamic 3D MR angiography of intra- and extracranial vascular malformations at 3T: a technical note. AJNR Am J Neuroradiol 2005;26:630–634.
17. Hans FJ, Reinges MH, Reipke P, Reinacher P, Krings T. Clinical applications of 2-D dynamic contrast-enhanced MR subtraction angiography in neurosurgery — preliminary results. Zentralbl Neurochir 2005;66:170–179.
18. Mori H, Aoki S, Okubo T, et al. Two-dimensional thick-slice MR digital subtraction angiography in the assessment of small to medium-size intracranial arteriovenous malformations. Neuroradiology 2003;45:27–33.
19. Nagaraja S, Capener D, Coley SC, et al. Brain arteriovenous malformations: measurement of nidal volume using a combination of static and dynamic magnetic resonance angiography techniques. Neuroradiology 2005;47:387–392.
20. Summers PE, Kollias SS, Valavanis A. Resolution improvement in thick-slab magnetic resonance digital subtraction angiography using SENSE at 3T. J Magn Reson Imaging 2004;20:662–673.
21. Warren DJ, Hoggard N, Walton L, et al. Cerebral arteriovenous malformations: comparison of novel magnetic resonance angiographic techniques and conventional catheter angiography. Neurosurgery 2001;48:973–982.
22. Nael K, Ruehm SG, Michaely HJ, et al. High spatial-resolution CE-MRA of the carotid circulation with parallel imaging: comparison of image quality between 2 different acceleration factors at 3.0 Tesla. Invest Radiol 2006;41:391–399.
23. Meckel S, Mekle R, Taschner C, et al. Time-resolved 3D contrast-enhanced MRA with GRAPPA on a 1.5-T system for imaging of craniocervical vascular disease: initial experience. Neuroradiology 2006;48:291–299.
24. Willinek WA, Gieseke J, Hadizadeh DR, et al. Contrast-enhanced supraaortic MRA at 3.0T using 8-channel and 16-channel neurovascular coils and parallel acquisition with acceleration factors ranging from 1 to 9. Proc Int Soc Magn Reson Med 2006;14:567.
25. Willinek WA, Gieseke J, von Falkenhausen M, et al. CE-3D MRA of the supraaortic arteries at 512 and 1024 matrix: the use of randomly segmented central k-space ordering (CENTRA). Proc Int Soc Magn Reson Med 2002;10.
26. Cashen TA, Carr JC, Shin W, et al. Intracranial time-resolved contrast-enhanced MR angiography at 3T. AJNR Am J Neuroradiol 2006;27:822–829.
27. Oesterle C, Strohschein R, Kohler M, Schnell M, Hennig J. Benefits and pitfalls of keyhole imaging, especially in first-pass perfusion studies. J Magn Reson Imaging 2000;11:312–323.
28. Xiong J, Fox PT, Gao JH. The effects of k-space data undersampling and discontinuities in keyhole functional MRI. Magn Reson Imaging 1999;17:109–119.
29. Mende KA, Froehlich JM, von Weymarn C, et al. Time-resolved, high-resolution contrast-enhanced MR angiography of dialysis shunts using the CENTRA keyhole technique with parallel imaging. J Magn Reson Imaging 2007;25:832–840.
30. Mazaheri Y, Carroll TJ, Du J, et al. Combined time-resolved and high-spatial-resolution 3D MRA using an extended adaptive acquisition. J Magn Reson Imaging 2002;15:291–301.
31. Korosec FR, Frayne R, Grist TM, Mistretta CA. Time-resolved contrast-enhanced 3D MR angiography. Magn Reson Med 1996;36: 345–351.
32. Fink C, Ley S, Kroeker R, Requardt M, Kauczor HU, Bock M. Time-resolved contrast-enhanced three-dimensional magnetic resonance angiography of the chest: combination of parallel imaging with view sharing (TREAT). Invest Radiol 2005;40:40–48.
33. Madore B, Pelc NJ. New approach to 3D time-resolved angiography. Magn Reson Med 2002;47:1022–1025.